AMERICAN SCIENTIFIC PUBLISHERS

Advanced Chemistry Letters
Vol. 1, pp. 1–7, 2014
(www.aspbs.com/acl)

ARTICLE

Development of Cobalt Based Non-Precious Electrocatalyst for Oxygen Reduction Reaction

C. Venkateswara Rao*, K. Muthukumar, L. Hima Kumar, and B. Viswanathan*

National Centre for Catalysis Research, Department of Chemistry, Indian Institute of Technology Madras, Chennai 600036, India

Co/N/rGO$_x$ electrocatalyst is prepared by pyrolyzing cobalt(II)tetramethoxyphenylporphyrin (CoTMPP) adsorbed on reduced graphene oxide (rGO$_x$) sheets and characterized using scanning electron microscopy, transmission electron microscopy, energy dispersive X-ray spectroscopy and X-ray photoelectron spectroscopy techniques. Characterization techniques depict the fine dispersion of Co/N active species on rGO$_x$ sheets. Electrocatalytic activity toward oxygen reduction reaction (ORR) is investigated by rotating disk electrode voltammetry. Kinetic analysis reveals that the ORR on Co/N/rGO$_x$ follows the four-electron pathway leading to water. Also preliminary studies are carried out to investigate the electrocatalytic nature of CoN$_4$ doped graphene substrate and its interaction with the oxygen molecule using density functional theory (DFT). This study shows that the oxygen molecule has a stronger bonding and tendency for dissociation on the substrates with CoN$_4$ active sites.

KEYWORDS: Co–N Clusters, N$_4$-Metal Chelate, Oxygen Reduction, Density Functional Theory, RDE Voltammetry.

1. INTRODUCTION

Carbon supported platinum is the active, efficient and applicable catalyst for oxygen reduction in fuel cells.[1, 2] However, the usage of high amount of Pt for oxygen reduction reaction (ORR) at cathode increases the cost of the device and hinders commercialization. Also, Pt electrocatalysts has several drawbacks such as high overpotential ($\geq$300 mV) and sluggish kinetics for ORR beside the cost issue.[3, 4] In recent years, there have been efforts to find suitable non-Pt based catalysts which exhibit the similar activity of Pt.[5, 6] Transition metal (especially iron or cobalt), nitrogen and carbon containing catalysts in the form of MN$_x$C$_y$ are one class of non-precious metal catalysts (NPMCs) for ORR.

Electrocatalysis of the ORR on transition metal macrocycle, cobalt(II) phthalocyanine (CoPc) adsorbed on carbon was reported for the first time by Jasinski.[7] Thereafter, several macrocyclic complexes were investigated as oxygen reduction electrodes for electrochemical devices.[8–10] All experimental evidences demonstrated that macrocyclic complexes of Fe and Co appear to be the best. However, they suffer from low electrochemical stability and decompose either via hydrolysis in the electrolyte or destruction of the macrocycle ring by peroxy intermediates generated during oxygen reduction.[11] The results were not satisfactory in terms of both the activity and stability of these Co and Fe chelates. Later several research groups reported that the heat-treatment of iron or cobalt macrocycles adsorbed on carbon support improves their activity and stability. Moreover, a variety of methods have been employed to prepare electrocatalysts containing iron or cobalt, nitrogen and carbon and exploited them as ORR electrodes.[12–27] It was concluded that the activity depends on the metal, the ligand and nature of support. Efforts have been devoted to determine the composition and the structure of the active sites formed upon pyrolysis. The most widely accepted model to explain the improvement in activity and stability is the formation of M-N$_x$ moiety on carbon matrix or simply MN$_x$C$_y$ clusters (M = Fe or Co) during the pyrolysis.[6, 12, 13, 25, 28] Among the investigated NPMCs, CoN$_x$C$_y$ species generated by the pyrolysis of Co–N$_4$ macrocycles adsorbed on carbon appears to be best one for ORR. But the activity is not enough for practical applications. This may be due to the existence of less number of active sites, large particle size and weak bonding interactions between the carbon and active species responsible for ORR. It has been known that the surface properties of the carbon influences dramatically the degree of dispersion of supported active species and in turns its catalytic activity. The results accumulated over the years indicate that there is a possibility of increasing activity by increasing the dispersion of cluster species on suitable carbon support such as carbon nanotubes, graphitic carbon nanofibers, and graphene.

*Authors to whom correspondence should be addressed.
Emails: vrao.chitturi@ymail.com, bvnathan@iitm.ac.in
Received: XX Xxxxx XXXX
Accepted: XX Xxxxx XXXX

ARTICLE

Recently, graphene has received tremendous scientific and technological interests with potential applications in various fields such as electronic devices, energy storage and conversion devices, solar cells, biosciences, and biotechnologies.[29,30] The unique properties of graphene, especially good electronic conductivity, surface area, mechanical and/or thermal stability, and durability makes it a promising electrode/electrode support material for fuel cell applications. Graphene has been used as a support for metal nanoparticles and its activity and durability toward various electrochemical reactions have been investigated. The enhanced performance observed with the graphene supported metal electrodes is attributed to the intrinsic graphitization degree of graphene and the enhanced metal-support interaction.[31–33]

In the present study, reduced graphene oxide (rGO_x) is used as a support for cobalt(II)tetramethoxy phenylporphyrin (CoTMPP) for the first time and the electrocatalytic performance of $Co/N/rGO_x$ electrocatalyst towards ORR has been investigated.

2. METHODS

2.1. Experimental Details

Reduced graphene oxide (rGO_x) was synthesized from commercial graphite powder in a two step process. First step involves the oxidation and/or exfoliation of graphite to graphite oxide (GO_x) by a Hummer's method[34] and second step involves the chemical reduction of GO_x to rGO_x by treatment with sodium borohydride at 353 K for 1 h followed by dehydration with concentrated sulfuric acid at 454 K for 12 h.[35] The composition (wt.%) of prepared rGO_x is determined to be C: 83.7, O: 12.4, H: 1.7 and N: < 0.5.

CoTMPP complex was synthesized according to the method described by Adler et al.[36] and adsorbed on rGO_x by dissolving the suitable amount of CoTMPP in N,N'-dimethylformamide followed by impregnation. Then the resultant suspension was filtered to remove the solvent and dried. It was then heat-treated at 1073 K for 2 h under Ar atm to prepare CoN_4C_x electrocatalyst. The nominal metal content in the catalyst was 5 wt.%.

2.2. Theoretical

DFT calculations for the bulk graphene, graphene substrates both in its pristine and in doped form and its interaction with Oxygen molecule were performed using the projector augmented wave (PAW) method[37,38] implemented in the Vienna *Ab-initio* Simulation Package (VASP-5.2.11).[39–41] GGA in the parameterization of Perdew, Burke and Ernzerhof[42,43] was used as approximation for the exchange and correlation functional. In addition, dispersion corrections were used that simulate the long range vdW interactions.[44,45] For bulk graphene two atom unit cell with the lattice values for $a = b =$ 2.465 Å was used which is obtained by fitting of energy versus volume curve and the obtained values matches to the reported values. To simulate the substrate-precursor interaction a $5 \times 5 \times 1$ supercell was used that provides a distance of ca. 10 Å between two adsorbates and avoids the lateral interaction. The vacuum was set large enough that provides ca. 20 Å and prevents the dipole–dipole interaction. All calculations were performed in the scalar relativistic approximation. A kinetic energy cut-of 400 eV was used and all ions were fully relaxed using a conjugate gradient scheme until the forces were less than 0.01 eV/A. In the geometry optimizations for the molecule and the surface models the Brillouin zone was sampled at the Γ point only. The adsorption energy (AE) was defined as $AE = E_{total} - (E_{substrate} + E_{adsorbate})$ where E_{total}, $E_{substrate}$, and $E_{adsorbate}$ are the energies of the combined system (adsorbate and cluster), of the cluster, and of the adsorbate molecule in the gas phase in a neutral state, respectively.

2.3. Characterization Techniques

X-ray diffraction (XRD) measurements were performed on a Siemens D5000 X-ray diffractometer using a Cu Kα source operated at 30 keV at a scan rate of 0.02 $^{\circ}s^{-1}$. Raman spectrum was recorded with a Renishaw In Via Raman microscope using $a \times 50$ objective lens at room temperature, with a 514.5 nm laser beam and 1,800 lines per mm grating. Surface area and pore size distribution of carbon black were investigated by Brunauer–Emmett–Teller (BET) analyses with nitrogen adsorption–desorption isotherms on a Carlo–Erba sorptometer (Model 1800) instrument at 77 K. Chemical composition of the materials was determined by Hereaus CHN analyzer. An inductively coupled plasma optical emission spectroscopic (ICP-OES) technique was employed to determine cobalt content in the prepared material. Scanning electron microscope (SEM) equipped with EDX (FEI, Model: Quanta 200) was used to observe the surface morphology and composition of the materials. Particle size was determined using transmission electron microscope (TEM, JEOL2100). X-ray photoelectron spectroscopy (XPS) measurements was carried out with Omicron nanotechnology instrument using an Al monochromatic X-ray ($h\nu = 1486.6$ eV).

Electrocatalytic activity of the material was investigated at room temperature by rotating disk electrode (RDE) voltammetry using a potentiostat (BAS100 electrochemical analyzer) connected to a three electrode cell assembled with catalyst coated glassy carbon (GC) disk as the working electrode, Ag/AgCl, 3.5 M KCl (+0.205 V vs. NHE) as the reference and Pt foil as the counter electrodes, respectively. Oxygen saturated 0.5 M H_2SO_4 was used as the electrolyte. The working electrode was fabricated as follows: catalyst ink was made by mixing 10 mg of catalyst with 0.6 mL of deionized water and 0.2 mL of a 5 wt% Nafion in alcohol-water solution (Aldrich) in an ultrasonic bath for 20 min. 5 μL of the ink was dropped onto a GC disk (6 mm diameter) and dried under Ar atmosphere. Current densities were normalized to the geometric area of the RDE disk (0.283 cm^2).

3. RESULTS AND DISCUSSION

Structural features of the rGO_x are examined using powder XRD and Raman spectroscopy techniques. XRD pattern (Fig. 1(a)) shows the characteristic (002) and (100)/(101) diffraction peaks at 2θ values around 25.4 and 43.1°, respectively. These peaks are indexed to the reflections of hexagonal graphite. The sharp diffraction peaks with high intensity indicates the crystalline nature of the material. The (002) diffraction peak at 25.4° corresponds to the interspacing between the graphene layers as 3.51 Å. A slight increase in the interlayer spacing from the normal value observed for graphite (3.34 Å) is ascribed to the presence of oxygen-containing functional groups bonded on both sides of the rGO_x sheets.[33] Raman spectrum recorded for the rGO_x is shown in Figure 1(b). As can be seen, it exhibited the characteristic D, G, and 2D peaks at ca. 1345, 1580 and 2697 cm^{-1} respectively.[33] The appearance of intense G peak indicates the graphitization of the rGO_x. The more intense D peak observed for rGO_x is due to the creation of defect sites by chemical treatment. The broad and less intense 2D peak observed at ca. 2697 cm^{-1} indicates that the rGO_x has 4–6 layers.[35] The peak centered at ca. 2930 cm^{-1} corresponds to the combination of the D and G peaks for graphene layers. Specific surface area of the rGO_x is determined using Brunauer–Emmett–Teller (BET) sorptometer and the corresponding isotherm is shown in Figure 1(c). The BET specific surface area of the rGO_x is calculated to be ca. 810 m^2/g. The combination of graphitization nature and good surface area of rGO_x would be beneficial for supporting metal clusters and improving electrochemical properties.

Elemental composition (wt%) of the purified CoTMPP ($C_{48}H_{36}N_4O_4Co$) complex is found to be C, 71.90; H, 4.41; N, 6.97 and Co, 7.49 and it is in good agreement with that of the calculated values. Also, the composition of heat-treated CoTMPP/rGO_x according to the bulk metal and N concentrations is determined to be $CoN_{3.1\pm0.2}$. Surface morphologies of the materials is studied by scanning electron microscopy (SEM) and transmission electron microscopy (TEM) and the corresponding images are shown in Figures 2 and 3, respectively. Micron size

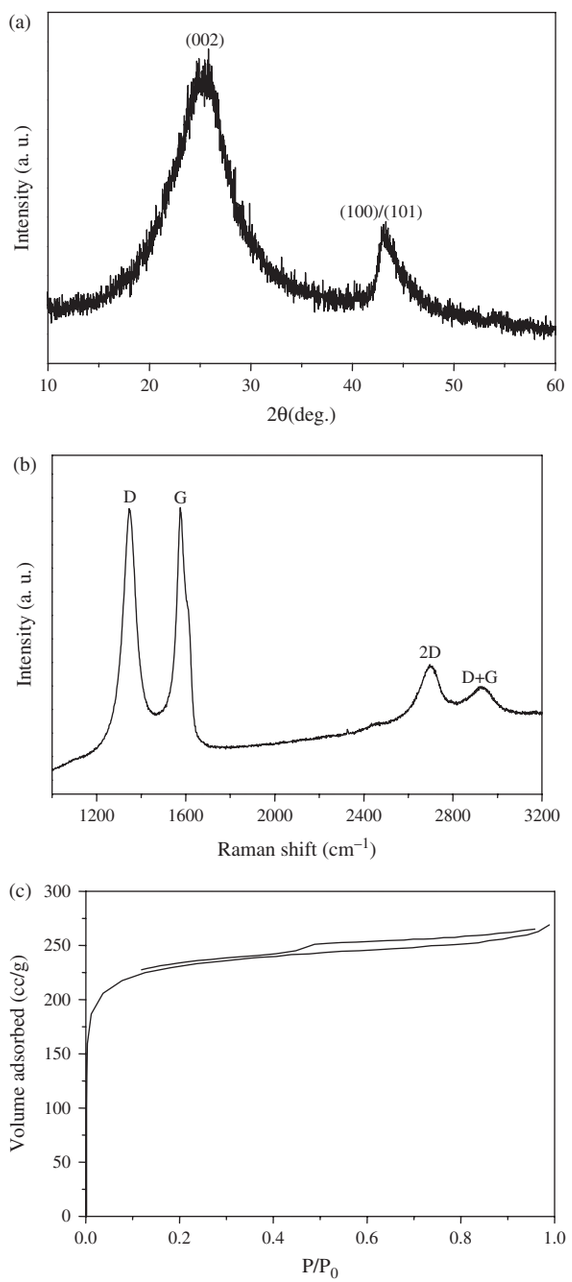

Fig. 1. (a) Powder XRD pattern, (b) raman spectrum and (c) nitrogen adsorption–desorption isotherm of reduced graphene oxide (rGO_x).

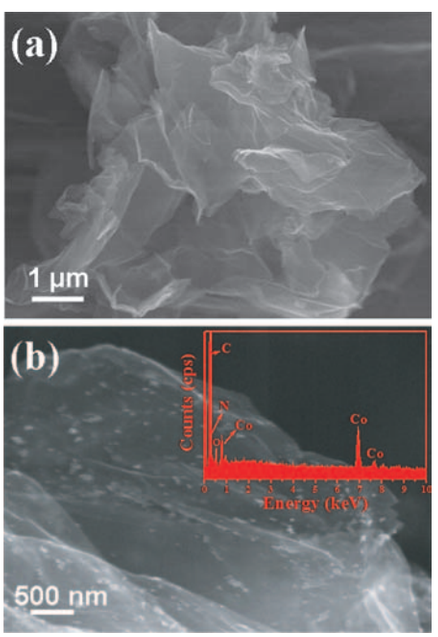

Fig. 2. SEM images of (a) rGO_x and (b) heat-treated CoTMPP/rGO_x at 1073 K. Inset in Figure 1(b) shows the corresponding EDX spectrum.

ARTICLE

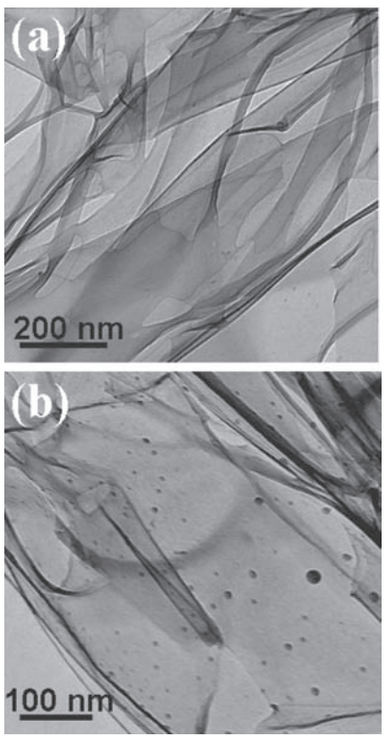

Fig. 3. TEM images of (a) rGO_x and (b) heat-treated CoTMPP/rGO_x at 1073 K.

corrugated and transparent rGO_x sheets can be seen from SEM and TEM images recorded for the rGO_x (Figs. 2(a) and 3(a)). SEM image of the heat-treated CoTMPP/rGO_x at 1073 K depicts the nano-sized particles anchored on the rGO_x sheets (Fig. 2(b)). The corresponding EDX pattern (shown in the inset in Fig. 2(b)) confirms the presence of Co, N, C and small amount of oxygen. High-magnification TEM image presented in the Figure 3(b) depicts the randomly distributed metallic clusters of average size 10 nm embedded in the rGO_x matrix. It may originate from interfacial bonds with the oxygenated groups of graphene surfaces which act as anchors for the supported clusters. The local EDX indicates that these tiny clusters are Co nanocrystals.

The studies performed on Co-based non-precious ORR catalysts impart that the presence of Co/N species at the surface plays an important role in the adsorption and reduction of molecular oxygen. To probe the nature of the species existed on the surface, XPS measurements are performed and the corresponding X-ray photoelectron (XP) narrow scan spectra in the Co 2p, N 1s, and C 1s regions are provided in Figure 4. The $Co2p_{3/2}$ peak observed at a binding energy of 780.3 eV is attributed to the existence of Co(II).[14] XP N1s spectrum consists of two peaks at binding energies of 398.3 and 401.2 eV characteristic of pyridinic-and graphitic-type nitrogen, respectively.[14] The occurrence of nitrogen atoms in two chemical environments was also observed for heat-treated cobalt macrocycles adsorbed on carbon.[5, 6, 14] The observed C1s peak at 284.5 eV mainly represents graphitic carbon.[35]

To evaluate the electrocatalytic ORR activity of Co/N/rGO_x, a thin-film electrode is fabricated and steady-state polarization curves are recorded at a scan rate of 5 mV/s over a range of rotation rates of 0–3600 rpm. Figure 5(a) shows the dependence of the oxygen reduction reaction activity as a function of potential and rotation rate. The increase in current density with the rotation rate can be observed. The steep increase in peak current at the potential of 0.85 V indicates the facile kinetics of oxygen reduction. The voltametric profiles are in good agreement with the literature reports and the ORR activity is imputed to the existence of greater number of $Co–N_4$ active species at the graphene surface.[12–14, 28] The onset potential for ORR (the potential where the current density increases to 20 $\mu A/cm^2$) on the catalyst was + 840 mV versus NHE. The overall current density (i) in

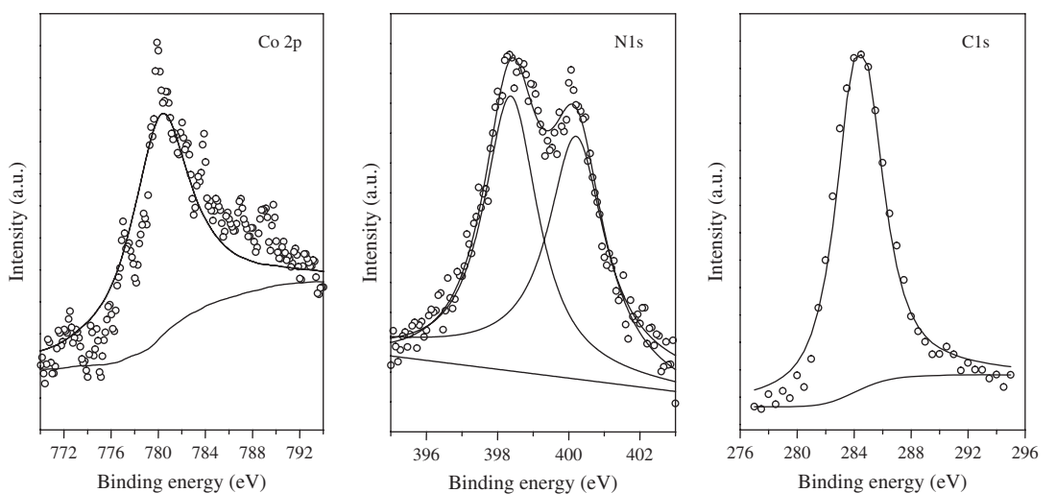

Fig. 4. Narrow scan XP $Co2p_{3/2}$, N1s and C1s spectra of the heat-treated CoTMPP/rGO_x at 1073 K.

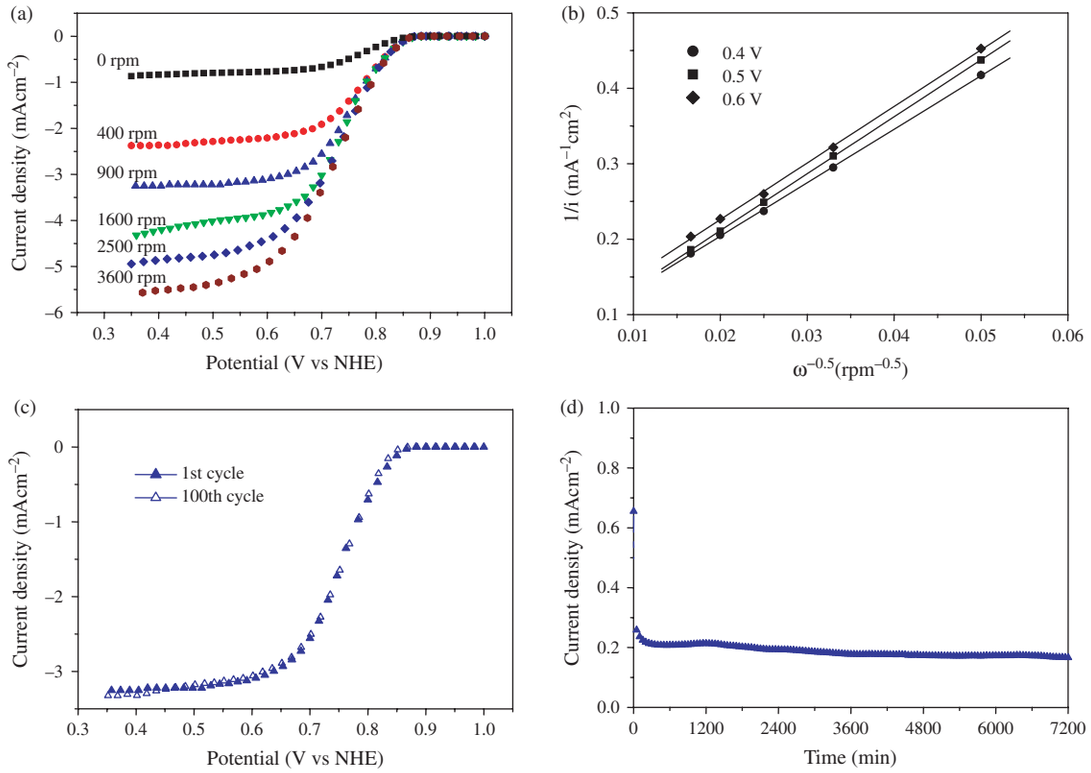

Fig. 5. (a) Polarization (I–V) curves at different rotation rate recorded in O_2-saturated 0.5 M H_2SO_4 for heat-treated CoTMPP/rGO$_x$ at 1073 K, scan rate–5 mV s^{-1}; (b) Corresponding K–L plot for the ORR on the catalyst at +0.4, +0.5 and +0.6 V versus NHE; (c) LSVs for the ORR at the heat-treated CoTMPP/rGO$_x$ catalyst before and after a continuous potentiodynamic swept for 100 cycles in O_2-saturated 0.5 M H_2SO_4; Scan rate–5 mV s^{-1} and rotation rate–900 rpm and (d) Current density-time plots of heat-treated CoTMPP/rGO$_x$ catalyst in O_2-saturated 0.5 M H_2SO_4 at +0.75 V versus NHE at rotation rate of 900 rpm.

the ORR via RDE is the resultant of contributions from the kinetic current density (i_k), diffusion limiting current density in the Nafion film covering the catalyst layer (i_f) and diffusion limiting current density through the solution boundary layer (i_d) according to the equation: $(1/i) = (1/i_k)+(1/i_f)+(1/i_d)$.[46, 47] Since the amount of Nafion in the electrode is small and the film resistance is sufficiently small (~0.01 mA^{-1}cm^2), the overall current density can be described as, $(1/i) = (1/i_k)+(1/i_d)$. The value for i_d can be represented as

$$i_d = 0.62n_eFACD^{2/3}\upsilon^{-1/6}\omega^{1/2}$$

where n_e is the number of electrons transferred in the reaction, F is the Faraday constant, A is the geometric area of electrode, C is the concentration of dissolved oxygen in the solution (1.26×10^{-3} M), D is the diffusion coefficient (1.9×10^{-5} cm^2 s^{-1}), υ is the kinematic viscosity (1.07×10^{-2} cm^2 s^{-1}) and ω is the electrode rotation rate. According to this equation, a plot of the inverse of the current density at constant potential versus $\omega^{-1/2}$ ought to result in a straight line with an intercept. To determine the number of electrons transferred in the reaction, the overall current density (i^{-1}) was plotted against the square root of angular velocity ($\omega^{-1/2}$) at different potentials and the corresponding Koutecky-Levich plot is shown in Figure 5(b). The slope defined by $0.62n_eFACD^{2/3}\upsilon^{-1/6}$ corresponds to the number of electrons transferred in the reaction (n_e) as ca. 3.7.

To investigate the stability of the Co/N/rGO$_x$ electrode, continuous potential cycling studies as well as chronoamperometry studies are performed and the corresponding plots are shown in Figures 5(c) and (d), respectively. As can be seen from the LSVs (Fig. 5(c)), no obvious decrease in the ORR activity is observed for Co/N/rGO$_x$ electrode after continuous 100 cycles. The current density-time plot (Fig. 5(d)) recorded at +0.75 V versus NHE and a rotation rate of 900 rpm also shows the stabilization in the current density for 2 h. The retained ORR activity at +0.75 versus NHE after continuous potentiodynamic scan for 100 cycles and the low degradation of ORR activity for a period of 2 h observed for the Co/N/rGO$_x$ electrode is likely due to the high crystallization degree of rGO$_x$ support, enhanced metal-nitrogen-graphene interaction and existence of greater number of Co–N_4 active centers on the graphene surface.

A general thought about the catalytic structure of CoTMPP for ORR is that it is built based on the core

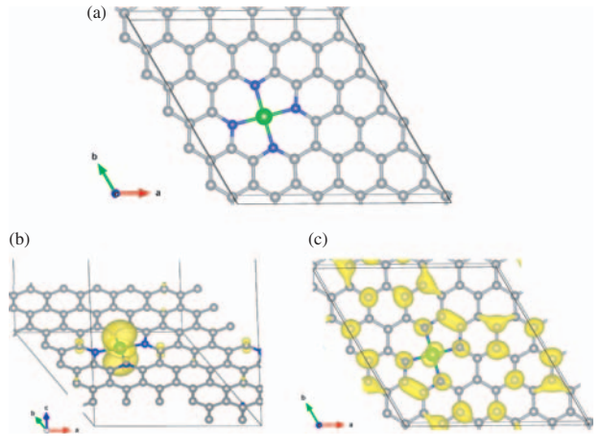

Fig. 6. (a) DFT optimized structure of CoN_4 doped graphene substrate and the frontier ((b) valence (c) conductance) bands. The isosurface value used is 0.001 e/Å^3 (Color code: Green corresponds to cobalt, blue to nitrogen and grey for carbon throughout this manuscript).

structure of CoTMPP (Co–N_4). To get more quantitative insights into the electrocatalytic nature of CoN_4C_x species for ORR, DFT calculations are carried out to investigate the interaction between the CoN_4C_x species and the oxygen molecule. The structure of DFT optimized substrate and the character of its frontier bands is shown in Figure 6. The charge density on the valence band is localized on the Co atom while it is delocalized on the conductance band. The oxygen molecule is placed on the substrate on several bonding sites (on-top of Co, N, and C, hollow and across the Co—N, C—N and C—C double bond etc.) and is relaxed subsequently. The resulting most stable configurations (Fig. 7) indicate that preferred O_2 bonding site on the substrate is on-top of the Co atom. We also observe that, irrespective of the initial binding sites, the O_2 molecule moves to on-top of the Co atom during geometry optimization and exhibits a significant stronger bonding (AE = −1.725 eV) compared to the pristine substrates (AE = −0.17 eV). The facile reduction is further illustrated by analyzing the bonding distance between Co—O and O—O atoms, where in the case of Co—N_4 graphenes these values are 1.872 and 1.295 Å compared to the pristine graphene with the distance of 2.9–3.01 and 1.25 Å respectively. According to the Klopman's concept of electrochemical reactivity,[48] frontier controlled electron transfer reactions occur when the frontier orbitals of the donor and acceptor have energy values close to each other. Since the O_2 molecule in its ground state possesses two unpaired electrons in a doubly degenerate π^* anti-bonding orbital (HOMO), reduction takes place by the transfer of electrons from the substrate to the molecular oxygen. This in fact could be further confirmed by the increase in the bader charges on the oxygen molecule by 0.45 e^-. The so formed adduct undergoes further reduction to give intermediate species like peroxide which can be decomposed/reduced further to give water.

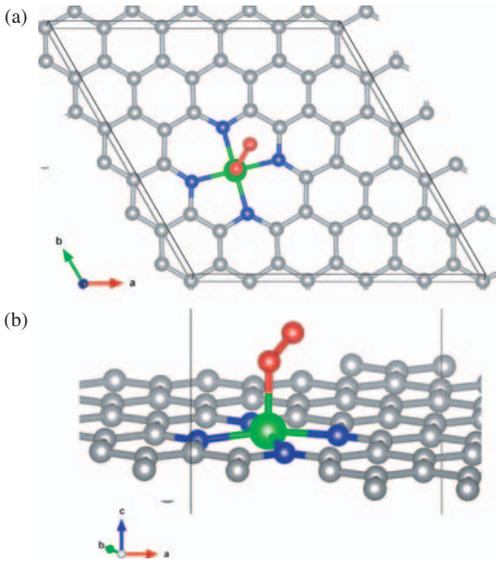

Fig. 7. Top and side views of most stable configuration of O_2 on CoN_4 doped graphene. O_2 prefers bonding to on-top of Co atom. (red balls correspond to oxygen).

4. SUMMARY

Well-dispersed metallic Co/N species on rGO_x sheets were prepared by pyrolyzing CoTMPP anchored graphene sheets. RDE voltammetry measurements indicate good oxygen reduction activity for the Co/N/rGO_x electrocatalyst. Kinetic analysis reveals that the number of electrons transferred in ORR process is approximately 4. The results also demonstrate the good stability of the Co/N/rGO_x electrocatalyst. The facile reduction of oxygen was attributed to the suitable energy level alignment that facilitates the charge transfer from CoN_4 doped graphene substrate to the π^* orbital of O_2.

References and Notes

1. B. Viswanathan and M. A. Scibioh (eds.), Fuel Cells–Principles and Applications, Universities Press (India) Private Limited, New Delhi (**2006**).
2. C. Venkateswara Rao and B. Viswanathan, *J. Phys. Chem. C* 114, 8661 (**2010**).
3. T. R. Ralph and M. P. Hogarth, *Platinum Met. Rev.* 46, 3 (**2002**).
4. H. A. Gasteiger, S. S. Kocha, B. Sompalli, and F. Wagner, *Appl. Catal. B: Environmental* 56, 9 (**2005**).
5. M. Lefèvre, E. Proietti, F. Jaouen, and J. P. Dodelet, *Science* 324, 71 (**2009**).
6. B. Rajesh and P. Zelenay, *Nature* 443, 63 (**2006**).
7. R. Jasinski, *Nature* 201, 1212 (**1964**).
8. H. Jahnke, M. Schönborn, and G. Zimmermann, *Top. Curr. Chem.* 61, 133 (**1976**).
9. J. P. Collman, P. Denisevich, Y. Konai, M. Maraocco, C. Koval, and F. C. Anson, *J. Am. Chem. Soc.* 102, 6027 (**1980**).
10. J. Zagal, M. Paez, A. A. Tanaka, J. R. dos Santos, and C. A. Linkous, *J. Electroanal. Chem.* 339, 13 (**1992**).
11. J. A. R. van Veen, J. F. Van Baar, and K. J. Kroese, *J. Chem. Soc. Faraday Trans I* 77, 2827 (**1981**).
12. R. W. Joyner, J. A. R. Van Veen, and W. M. H. Sachtler, *J. Chem. Soc. Faraday. Trans. I* 78, 1021 (**1982**).

ARTICLE

13. B. Van Wingerden, J. A. R. van Veen, and C. T. J. Mensch, *J. Chem. Soc. Faraday. Trans. I* 84, 65 (**1988**).
14. G. Lalande, R. Cote, G. Tamizhmani, D. Guay, J. P. Dodelet, L. Dignard-Baley, L. T. Weng, and P. Bertrand, *Electrochim. Acta* 40, 2635 (**1995**).
15. M. Ladouceur, G. Lalande, D. Guay, J. P. Dodelet, L. Dignard-Bailey, M. L. Trudeau, and R. Schulz, *J. Electrochem. Soc.* 140, 1974 (**1993**).
16. G. Faubert, G. Lalande, D. Cote, D. Guay, J. P. Dodelet, L. T. Weng, P. Bertrand, and G. Denes, *Electrochim. Acta* 41, 1689 (**1996**).
17. P. Goúerec, M. Savy, and J. Riga, *Electrochim. Acta* 43, 743 (**1998**).
18. P. N. Subramanian, P. S. Kumaraguru, H. Colon-Mercado, H. Kim, N. B. Popov, T. Black, and A. D. Chen, *J. Power Sources* 157, 56 (**2006**).
19. R. Yang, A. Bonakdarpour, E. B. Easton, B. Stoffyn-Egli, and J. R. Dahn, *J. Electrochem. Soc.* 154, A275 (**2007**).
20. B. Viswanathan, C. Venkateswara Rao, and U. V. Varadaraju, *PEPEEF* 43 (**2006**).
21. M. Yuasa, A. Yamaguchi, H. Isuki, K. Tanak, M. Yamamoto, and K. Oyizu, *Chem. Mater.* 17, 4278 (**2005**).
22. A. L. Mohana Reddy, N. Rajalakshmi, and S. Ramaprabhu, *Carbon* 46, 2 (**2008**).
23. S. Ye and K. Ashok Vijh, *Int. J. Hydrogen Energy* 30, 1011 (**2005**).
24. A. H. C. Sirk, S. A. Campbell, and V. I. Birss, *Electrochem. Solid-State Lett.* 8, A104 (**2005**).
25. M. Lefèvre, J. P. Dodelet, and P. Bertrand, *J. Phys. Chem. B* 109, 16718 (**2005**).
26. M. C. M. Alves, J. P. Dodelet, D. Guay, M. Ladouceur, and G. Tourillon, *J. Phys. Chem.* 96, 10898 (**1992**).
27. E. B. Easton, R. Yang, A. Bonakdarpour, and J. R. Dahn, *Electrochem. Solid-State Lett.* 10, B6 (**2007**).
28. M. Lefèvre, P. Bertrand, and J. P. Dodelet, *J. Phys. Chem. B* 104, 11238 (**2000**).
29. A. K. Geim and K. S. Novoselov, *Nat. Mater.* 6, 183 (**2007**).
30. A. K. Geim, *Science* 324, 1530 (**2009**).
31. Y. Shao, S. Zhang, C. Wang, Z. Nie, J. Liu, Y. Wang, and Y. Lin, *J. Power Sources* 195, 4600 (**2010**).
32. C. Venkateswara Rao and Y. Ishikawa, *J. Phys. Chem. C* 115, 21963 (**2011**).
33. C. V. Rao, A. L. M. Reddy, Y. Ishikawa, and P. M. Ajayan, *Carbon* 49, 931 (**2011**).
34. W. S. Hummers and R. E. Offeman, *J. Am. Chem. Soc.* 80, 1339 (**1958**).
35. W. Gao, L. B. Alemany, L. Ci, and P. M. Ajayan, *Nat. Chem.* 1, 403 (**2009**).
36. A. D. Adler, F. R. Longo, F. Kampas, and J. Kim, *J. Inorg. Nucl. Chem.* 32, 2443 (**1970**).
37. P. E. Blochl, *Phys. Rev. B* 50, 17953 (**1994**).
38. G. Kresse and D. Joubert, *Phys. Rev. B* 59, 1758 (**1999**).
39. G. Kresse and J. Furthm⋆uller, *Computational Materials Science* 6, 15 (**1996**).
40. G. Kresse and J. Hafner, *Phys. Rev. B* 47, 558 (**1993**).
41. G. Kresse and J. Hafner, *Phys. Rev. B* 49, 14251 (**1994**).
42. J. P. Perdew, K. Burke, and M. Ernzerhof, *Phys. Rev. Lett.* 77, 3865 (**1996**).
43. J. P. Perdew, K. Burke, and M. Ernzerhof, *Phys. Rev. Lett.* 78, 1396 (**1997**).
44. S. Grimme, *J. Comp. Chem.* 27, 1787 (**2006**).
45. X. Wu, M. C. Vargas, S. Nayak, V. Lotrich, and G. Scoles, *J. Chem. Phys.* 115, 8748 (**2001**).
46. J. Koutecky and V. G. Levich, *Zh. Fiz. Khim.* 32, 1565 (**1958**).
47. T. J. Schmidt, U. A. Paulus, H. A. Gasteiger, N. Alonso-Vante, and R. J. Behm, *J. Electrochem. Soc.* 147, 2620 (**2000**).
48. G. Klopman, *J. Am. Chem. Soc.* 90, 223 (**1968**).

ARTICLE